Shifting the Burden of Selectivity from Chemical to Physical Separation Processes via Selective Sulfidation

Shifting the Burden of Selectivity from Chemical to Physical Separation Processes via Selective Sulfidation

Caspar Stinn[1] and Antoine Allanore[1*]

[1] Massachusetts Institute of Technology, Department of Materials Science and Engineering, 77 Massachusetts Avenue, Cambridge, MA 20139, USA
[*] Corresponding Author: allanore@mit.edu

Abstract

Increasing demand for critical metallic elements for sustainability applications motivates new approaches in primary and secondary production to handle falling ore grades and increasingly-convoluted recycling streams. Separation of elements in distinct phases is generally less energy intensive than separation of elements substituted in a single phase, a phenomenon referred to in primary extraction as the "mineralogical barrier". Engineered materials leverage element substitution within single phase solutions to achieve target material performance. This results in large energy requirements during end of life recycling to selectively recover, via chemical separation, the target elements contained within a single phase. Herein, we present selective sulfidation as a novel, pyrometallurgical pretreatment to selectively partition target elements from a single phase into distinct, separate phases. We find such approach may support more competitive physical separation of difficult to isolate elements that previously required separation via complete hydrometallurgical dissolution and aqueous-organic liquid-liquid solvent extraction. We demonstrate selective sulfidation as applied to end-of-life magnet, battery, and copper slag recycling as a means to shift the burden of selective separation from chemical to physical processes.

Keywords: Sulfidation, Recycling, Lithium-ion batteries, Rare-earth magnets, Slag, Copper smelting, Physical separation, Pyrometallurgy, Mineralogical barrier

Introduction

The electrification of sectors ranging from transportation[1] to heavy industry[2] stimulates growing demand for the materials needed to establish infrastructure based on renewable technologies, spanning from base elements such as copper and nickel[3] to specialty elements such as the rare earths[4]. Meeting growing demand for these critical metallic elements motivates strategies for expanding both primary and secondary production[5,6]. Addressing growing demand in primary production requires designing processes to handle lower mineral and concentrate grades[7], while continuing to tackle the high emissions and energy usage characteristic of both conventional pyrometallurgy and hydrometallurgy[8]. Meanwhile, recycling of materials from secondary feedstocks requires the reprocessing of engineered materials designed with mixed-metal compounds and solid solutions[9–11]. In practice, primary and secondary production are often intertwined due to the role primary smelters play in recycling both base and rare elements[12,13], and the similar thermodynamic and energetic challenges faced in optimizing physical and chemical separations for recovery of elements from complicated, mixed-element feedstocks[12–14].

In primary production, metallic element sources can be grouped into two categories: those that exist as the dominant cationic species in a single mineral or phase, and those that exist as minor components in phases or minerals via atomic substitution. This distinction between physical and chemical mixtures of natural minerals is termed the "mineralogical barrier"[15]. Across the mineralogical barrier, energy requirements and costs are higher for chemical separation of elements versus physical separation[16]. Secondary sources of materials likewise exhibit their own "mineralogical barrier" between systems where target elements exist as physically-separable entities – such as cathode separation from casing materials in batteries – and systems where target elements are engineered to be in solid solution or mixed metal compounds. The latter requires chemical separations – such as cobalt separation from manganese in nickel-manganese-cobalt (NMC) oxide battery cathode chemistries[17]. While study of the mineralogical barrier does not replace detailed life cycle assessment with well-defined system boundaries tailored to individual processes or materials, it serves as a useful generalization of energy use trends in materials extraction.

Theoretical and practical mineralogical barriers are compared in Figure 1 as a function of product grade in the material feedstock, with the grades of critical elements from recycled magnet, battery, and slag sources noted[18–20]. The theoretical mineralogical barrier for a target element grade in a material feedstock may be determined by the difference in the minimum work required to chemically extract that component from a single-phase mixture, derived from the ideal Gibbs energy of mixing at a temperature of 25 °C, and the minimum work required for physical liberation. This can be assessed for one spherical grouping of particles from the bulk material, derived using crack resistance energy[21] and the King liberation model[22,23]. Meanwhile, a practical mineralogical barrier may be determined by comparing the actual energy input for comminution and physical separations in mineral concentrate

production to that of leaching and solvent extraction in chemical separations. For physical separation processes, energy for grinding using high intensity stirred mills and physical separation via froth flotation as a function of liberated particle size is sometimes available[24]. Here it is taken from zinc sulfide concentrate production data[25], chosen as a model system due to the wide range of liberation sizes practiced in the industry. Energy requirements for high pressure acid leaching (HPAL), solvent extraction (SX), and electrowinning (EW) for copper and nickel[8] are used as model systems for simple hydrometallurgical chemical separations. They provide a fair proxy due to the limited number of solvent extraction stages required for separation[12,13]. Energy requirements for rare earth element acid roasting, leaching, solvent extraction (SX), and compound precipitation are used as a model system for chemical separations requiring numerous hydrometallurgical separation stages[14].

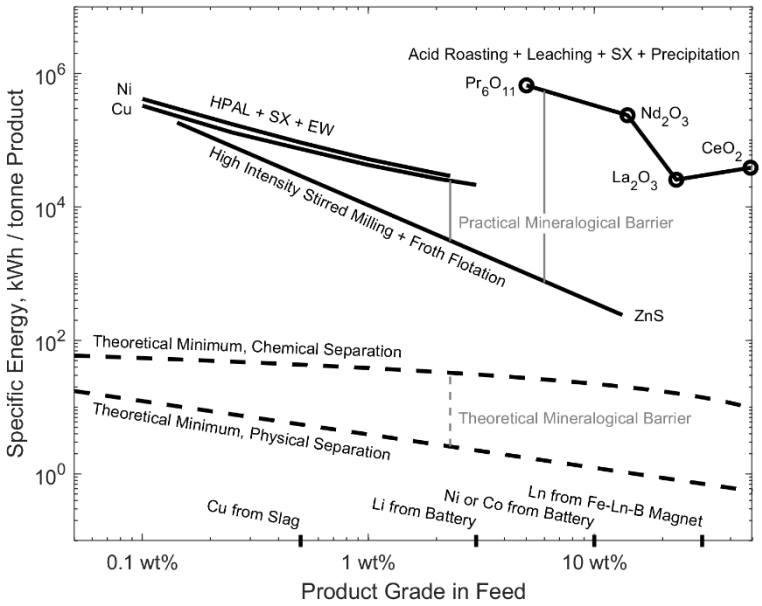

Figure 1: Calculated theoretical and practical mineralogical barriers suggests that physical separations are generally less energy intensive than chemical separations at sufficiently high target element grades in feedstocks. If the burden of selectivity can be shifted from chemical to physical separation processes via a suitable, energy efficient pretreatment, significant energy savings in materials separation are possible at grades relevant for recovery of critical elements from recycled magnet, battery, and slag sources. (HPAL: high pressure acid leaching. SX: solvent extraction. EW: electrowinning. Ln: lanthanide).

The practical mineralogical barrier between physical and simple chemical separations is observed to decrease in relative magnitude with decreasing material grade. At a grade of approximately 0.1 wt%, the difference in energy requirements for material separation via physical and simple hydrometallurgical methods becomes negligible. This correlation is consistent with the conventional wisdom that when minerals become too fine-grained or low grade, leaching and hydrometallurgical processing is necessary for product recovery due to decreasing comminution efficiency at decreasing liberation sizes. Meanwhile, with increasing material grade, the energy reduction of physical separations over chemical separations is readily apparent. For example, at feedstock grades of 0.5 wt%, 3 wt%, 10 wt%, and 30 wt%, corresponding to copper recycling from slag, lithium recycling from lithium ion batteries, nickel or cobalt recycling from lithium ion batteries, and lanthanide recycling from iron-lanthanide-boron magnets respectively, the practical barrier is approximately 45,000 kWh, 19,000 kWh, 11,000 kWh, and 6,000 kWh respectively per tonne of product, or 225 kWh, 570 kWh, 1100 kWh, and 1800 kWh respectively per tonne of feed. For pretreatment processes that enable physical separation, this can be viewed as an energy budget, effectively a budget for conversion cost since energy use remains one of the largest contributors to operating cost in minerals processing[26]. For reference, the energy burden of copper slag cleaning in a flash furnace is approximately 100 kWh per tonne of feed[13], and nickel smelting in an electric arc furnace is approximately 500 kWh per tonne of feed[12]. Therefore, for high-grade feedstocks where target elements are trapped in solid solutions, such as many secondary sources of critical elements, a simple pyrometallurgical pretreatment is attractive. It must facilitate cracking of solid solutions into physically separable phases, so that the burden of selectivity for the product elements is shifted from chemical to physical separation processes.

Pyrometallurgical roasting processes based on sulfide chemistry are promising pretreatments for physical separation. They offer to selectively partition target metallic elements from mixed oxide phases into sulfide phases[27–33], allowing for liberation and physical separation based on the numerous differences in the physical properties between oxides and sulfides[13]. Sulfidation pretreatments for primary copper and nickel processing have been successfully performed at industrial scales[12,34], and are predicted to require low energy inputs due to the exothermic nature of oxide sulfidation reactions[24]. Herein, we present a thermodynamic framework for predicting selectivity in sulfidation. We then demonstrate selective sulfidation as a pretreatment to promote metallic element

recovery from rare earth magnets, lithium ion batteries, and copper slag, as an avenue to shift the energy burden of selectivity in metal recovery from chemical to physical separation methods.

Thermodynamic Framework for Selective Sulfidation

Formation of a sulfide from an oxide, oxysulfide, or sulfate may be described by the following pyrometallurgical anion-exchange reaction, where M is a metallic element and ω, ϕ, υ, τ, and σ define the reaction stoichiometry:

$$\frac{4\tau}{2\omega\sigma+\phi\tau-2\upsilon\tau} M_\omega O_\phi S_\upsilon + S_2 = \frac{4\omega}{2\omega\sigma+\phi\tau-2\upsilon\tau} M_\tau S_\sigma + \frac{2\phi\tau}{2\omega\sigma+\phi\tau-2\upsilon\tau} SO_2 \quad (1)$$

Elemental sulfur is chosen as the gaseous sulfidizing agent due to its low cost[35] and the fact that the other commonly-used gaseous sulfidizing agents, hydrogen sulfide and carbon disulfide, are known in the catalyst industry to be non-selective in their sulfidation of oxides[36]. At thermodynamic equilibrium, the activities of the oxide, oxysulfide, or sulfate reactant ($a_{M_\omega O_\phi S_\upsilon}$) and the sulfide product ($a_{M_\tau S_\sigma}$) are related to a stoichiometry-dependent ratio (ψ) of the sulfur and sulfur dioxide partial pressures (P_{S_2} and P_{SO_2} respectively) via the standard Gibbs energy of reaction ($\Delta_r G°$), gas constant (R), and absolute temperature (T):

$$\log_{10}\left(e^{\frac{\Delta_r G^\circ}{RT}}\right) + \log_{10}\left(\frac{a_{M_\tau S_\sigma}^{\frac{4\omega}{2\omega\sigma+\phi\tau-2\upsilon\tau}}}{a_{M_\omega O_\phi S_\upsilon}^{\frac{4\tau}{2\omega\sigma+\phi\tau-2\upsilon\tau}}}\right) = \log_{10}\left(\frac{P_{S_2}}{P_{S_2}^{\frac{2\phi\tau}{2\omega\sigma+\phi\tau-2\upsilon\tau}}}\right) = \psi \quad (2)$$

In turn, ψ describes from both pure compound behavior (ψ_{rxn}) and solution behavior (ψ_{sol}), where activities raised to their stoichiometric power are abbreviated by $A_{M_\omega O_\phi S_\upsilon}$ and $A_{M_\tau S_\sigma}$.

$$\log_{10}\left(e^{\frac{\Delta_r G^\circ}{RT}}\right) = \psi_{rxn} \quad (3)$$

$$\log_{10}\left(\frac{a_{M_\tau S_\sigma}^{\frac{4\omega}{2\omega\sigma+\phi\tau-2\upsilon\tau}}}{a_{M_\omega O_\phi S_\upsilon}^{\frac{4\tau}{2\omega\sigma+\phi\tau-2\upsilon\tau}}}\right) = \log_{10}\left(\frac{A_{M_\tau S_\sigma}}{A_{M_\omega O_\phi S_\upsilon}}\right) = \psi_{sol} \quad (4)$$

Eqs 1-4 can be compiled for all metal elements, assuming the data for and identity of $M_\omega O_\phi S_\upsilon$ and $M_\tau S_\sigma$ are known. ψ_{rxn} for chemistries studied herein, calculated using FactSage 8.0 supplemented with literature data[37], and the relative scale of ψ_{sol}, are depicted in Figure 2. ψ, ψ_{rxn}, and ψ_{sol} may be related to stoichiometric-independent ratios of the sulfur and sulfur dioxide partial pressures via the Gibbs phase rule by employing the formalism of Pourbaix[38] or Kellogg[39]. Selective sulfidation of target elements from a single phase can lead to the precipitation of distinct, physically-separable sulfide phases ($M_\tau S_\sigma$) from the surrounding matrix, as a result of the natural immiscibility of oxides, oxysulfides, sulfates, and sulfides[40–42]. When differences in ψ_{rxn} outweigh differences in ψ_{sol} between target elements, selectivity in sulfidation is well-captured by the behavior of the pure compounds. When differences in ψ_{rxn} are comparable to or outweighed by differences in ψ_{sol},

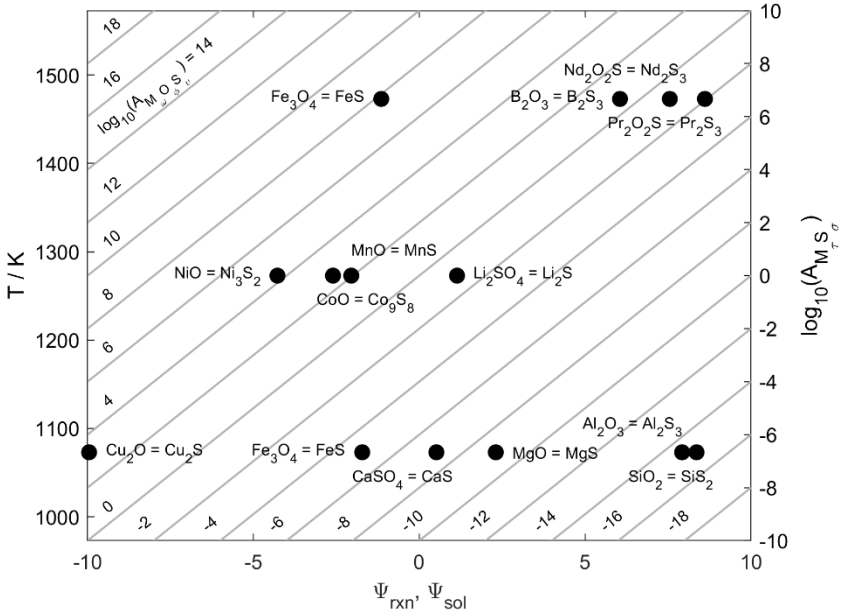

Figure 2: Sulfidation series for relevant chemistries considered herein, with the relative contributions from pure compound (ψ_{rxn}) and solution effects (ψ_{sol}) to the effective sulfur to sulfur dioxide ratio required for sulfidation to occur (ψ), as described in Eqs. 1-4.

knowledge of solution behavior is required to describe sulfidation selectivity. Unsurprisingly, the relative ease of sulfidation of oxides roughly follows the Goldschmidt geochemical classification of elements[43], with the oxides of chalcophile and siderophile elements generally sulfidizing at lower ψ_{rxn} than the oxides of lithophiles. A notable exception are the alkali and heavy alkaline earth oxides of calcium, strontium, and barium, which exhibit more moderate ψ_{rxn} than other lithophiles due to their natural propensity for sulfate formation[44], occurring at ψ_{rxn} intermediate to oxide or sulfide stabilization.

For many challenging materials separations, elements requiring energy-intensive chemical separation exhibit stark differences in ψ_{rxn}, such as iron-neodymium in magnet recycling, nickel-cobalt in battery recycling, and copper-silicon in slag recycling (Figure 2). Therefore, sulfide chemistry is a promising approach to shift the burden of selectivity in separation from expensive chemical methods to less energy-intensive physical methods. In the following sections, we demonstrate selective sulfidation as applied to rare earth magnet recycling[9], lithium ion battery recycling[10], and metal recovery from copper slags[20] to overcome the practical mineralogical barrier (Figure 1) to chemical and dilute physical separations for recycling of high-grade elements from engineered materials.

Selective Sulfidation for Rare Earth Magnet Recycling

Rare earth element magnets based on iron-lanthanide-boron chemistry are essential for advanced sustainability and electronic applications, ranging from renewable power generation to electric vehicles[4]. The supply of critical and strategically-significant lanthanide elements remains problematic due to environmentally unsustainable production[45], a lack of geographic diversity in processing infrastructure that is further confounded by illegal mining operations[46], and the rare earth element balance problem[6] – a mismatched supply and demand of different lanthanide coproducts with respect to their natural abundances. Recycling of high-demand lanthanides, such as neodymium, can lower the environmental impact of processing, decentralize rare earth element production, and selectively supplement the supply of disproportionately demanded lanthanide elements[47]. As shown in Figure 1, end of life rare earth magnets contains approximately 30 wt% lanthanides, with a neodymium grade higher than that of natural concentrate. Due to the similarity in electronic structure between lanthanides and the resulting difficulty in separation[14], the mineralogical barrier between chemical and physical separation processes is higher than that of base metals, with the energy burden of conventional chemical separation predicted to be on the order of 100x larger than an equivalent physical separation process at a lanthanide grade of 30 wt% . Numerous hydrometallurgical[18], pyrometallurgical[48], and liquid metal[49] processes have been explored for the chemical separation of elements from rare earth magnet materials, yet current recycling processes of both end of life magnets and production waste is complicated by the presence of oxide impurities[9,48]. Selective anion exchange pretreatments utilizing boron chemistry have been shown to facilitate physical separation of rare earth elements from one another for primary mineral processing[50], but such an approach has never been attempted with sulfide chemistry. As illustrated by ψ_{rxn} in Figure 2, at a sulfur to sulfur dioxide ratio on the order of 10:1, iron, rare earth elements, and boron are predicted to be stable in distinct sulfide, oxysulfide, and oxide phases respectively. Indeed, oxide-sulfide anion exchange chemistry is a thermodynamically promising pretreatment for facilitating selective recovery of lanthanides from rare earth magnet waste via physical separation.

To demonstrate selective sulfidation as a pretreatment to separate iron from lanthanides in rare earth magnet waste, nickel-plated iron-lanthanide-boron magnets (Ni-plated Fe-Nd-Pr-Dy-B, Grade N45, 6.25mm x 6.25mm x 6.25mm, McMaster-Carr) were heated under air at 500 °C to demagnetize, crushed to a particle size of 90-212 μm, then calcined under air at 1000 °C for 5 hours in a boron nitride crucible. The brittle iron-lanthanide-boron magnet was separated from the ductile nickel coating during comminution. The calcined rare earth oxide was reground to a particle size of 90-212 μm, then sulfidized at a scale of 2 g at 1200°C for one hour using vaporized elemental sulfur (S_x, 99.5% purity, Acros Organics) as a sulfur source, at a sulfur partial pressure of approximately 0.1 atm. The sulfur to sulfur dioxide ratio was set at approximately 10:1 following methods and reactor design described previously[33].

Figure 3 illustrates optical (dark field) microscopy and SEM/EDS (SEM: JEOL JSM-6610LV, JEOL Ltd., EDS: Sirius SD detector, SGX Sensortech Ltd.) element maps detailing oxygen, sulfur, iron, neodymium, and praseodymium distribution in the sulfidized product. As shown in Figure 3, iron partitioned to a sulfide phase, whereas neodymium and praseodymium remained as oxides (Figure 3), with product phases on the order of 20-100 μm in size and large enough for effective liberation[22,23] and physical separation using standard industrial mineral processing methods[25,51]. Boron, not shown in Figure 3, was also observed to partitioned to the oxide phase. The suppression of thermodynamically-predicted rare earth oxysulfide formation may be due to sluggish sulfidation kinetics for rare earth oxides, or due to solution effects (ψ_{sol}) stemming from compound-forming interactions between lanthanide and boron oxides[50,52]. Further research on lanthanide oxide sulfidation kinetics and iron-

lanthanide-boron-oxygen-sulfide solution thermodynamics is necessary to design sulfidation pretreatments for physical separation of individual lanthanides. Our preliminary results demonstrate that selective sulfidation is a technically-viable pretreatment to facilitate the physical separation of iron from lanthanide elements in rare earth magnet waste. The burden of selectivity for iron and lanthanides in rare earth magnet recycling may therefore by shifted across the mineralogical barrier from chemical separations to physical separations using a sulfidation pretreatment. In the following section, we apply a similar selective sulfidation process to overcome the mineralogical barrier in lithium ion battery recycling.

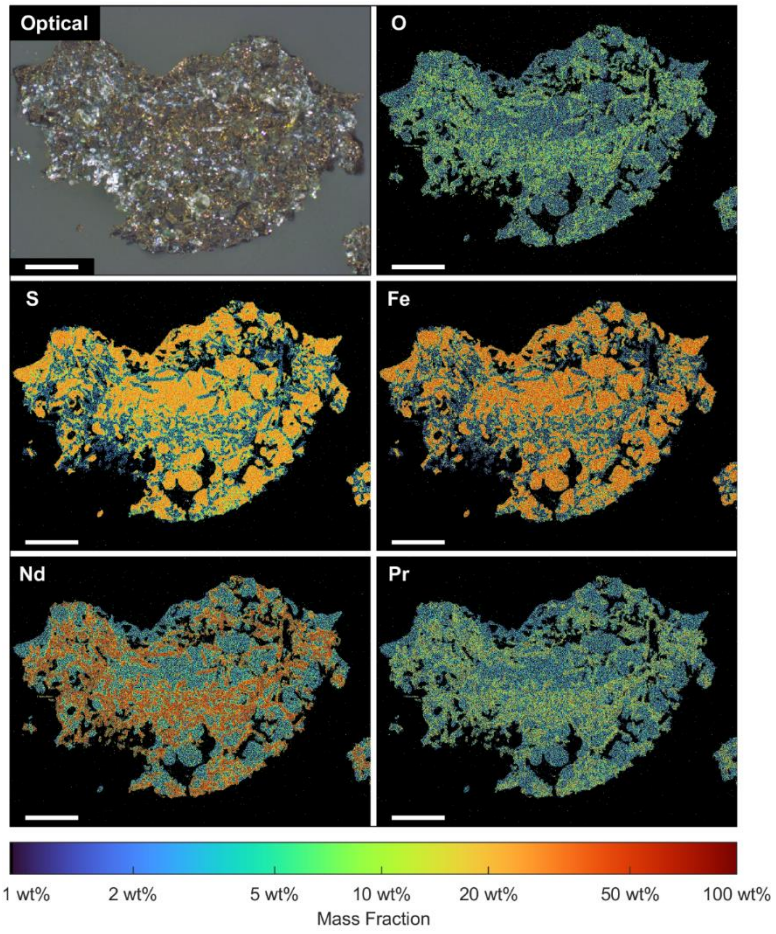

Figure 3: Selective sulfidation of calcined, de-coated iron-neodymium-boron magnet nucleates distinct iron sulfide and rare earth oxide phases on the order of 20-100 µm in size, as illustrated via EDS mapping for the region shown in the optical image, large enough for liberation of Fe and Nd-Pr via comminution and physical separation with optimization of phase growth and coarsening behavior. Scale bars correspond to 200 µm. (Color images available online).

Selective Sulfidation for Lithium-Ion Battery Recycling

As electrification of the transportation sector continues, effective recycling of lithium ion battery materials from electric vehicles is critical to minimizing energy use in their production[53]. Furthermore, the rapidly increasing demand for battery elements runs the risk of overwhelming geopolitically-uncertain supply chains for critical components[5]. In their current form, lithium ion batteries largely rely on cathodes engineered from solid solutions or mixed metal compounds of lithium, nickel, manganese, and cobalt (NMC) oxide [10,11]. While recycling methods based on physical separation for direct reuse have been explored, the constantly evolving state of the art for battery chemistries motivates hydrometallurgical and pyrometallurgical approaches that allow for recovery of pure components[1,17], in particular lithium, nickel, and cobalt compounds. In end of life lithium ion batteries, the average lithium grade is on the order of 3 wt%, whereas nickel and cobalt grades are on the order of 5-15 wt% depending on the cathode chemistry[19]. At these grades, a practical mineralogical barrier likely exists between physical and chemical methods of element recovery, with chemical separation predicted to require 10x-20x more energy than an equivalent physical separation process (Figure 1). Significant energy savings in recycling may therefore be possible thanks to the use of a low-energy pretreatment, such as sulfidation, to shift the burden of selectivity for lithium, nickel, and cobalt from chemical to physical separation processes.

Sulfidation chemistry has previously been considered to facilitate selective metallic element recovery from end of life lithium ion batteries via leaching, molten sulfide electrolysis, and physical separation[33,54,55]. From ψ_{rxn} in Figure 2, at the 10:1 sulfur to sulfur dioxide ratio lithium is predicted to be stable as a sulfate, with nickel, manganese, and cobalt stable as sulfides. The relative contributions of ψ_{rxn} and ψ_{sol} to ψ are unknown however due to mixed metal compound formation between lithium and NMC oxides[10,11] and the unexplored thermodynamics of the lithium-nickel-manganese-cobalt-oxygen-sulfur system. Herein, we explored selective sulfidation for 2 g of simulated NMC oxide cathode material ($LiNi_{1/3}Mn_{1/3}Co_{1/3}O_2$ solid solution, 98% purity, Sigma Aldrich) at 1000 °C for one hour using vaporized elemental sulfur (S_x, 99.5% purity, Acros Organics) as a sulfur source. The sulfur

partial was approximately 0.1 atm with a 10:1 sulfur to sulfur dioxide molar ratio, following methods and reactor design described previously[33].

Figure 4 show the SEM/EDS (SEM: JEOL JSM-6610LV, JEOL Ltd., EDS: Sirius SD detector, SGX Sensortech Ltd.) backscattered electron composition (BEC) image of and element maps detailing oxygen, sulfur, cobalt, manganese, and nickel distribution in the sulfidized lithium ion battery material. As depicted in Figure 4, sulfidation was indeed performed selectively, with the formation of distinct nickel-rich and cobalt-rich sulfide phases, with some solubility for oxygen, on the order of 100-200 μm in size, large enough for effective liberation[22,23] and physical separation using standard industrial mineral processing methods[25,51]. Meanwhile, instead of manganese sulfide as predicted from Figure 2, an under-sulfidized manganese-rich oxysulfide phase is formed; whether this phase is in fact an oxysulfide[56], oxysulfate[56], sulfatosulfide[56], or mixed oxide/sulfate/sulfide[56] is indiscernible from SEM/EDS element mapping in Figure 4. XRD analysis of the sulfidized product suggests the presence of some manganese sulfide, however oxysulfides of manganese may show poor crystallinity[57], so the precise nature of the manganese oxysulfide product phase remains unclear. While lithium is not visible via SEM/EDS, the presence in Figure 4 of oxygen-sulfur-rich regions lacking significant amounts of nickel, manganese, or cobalt, denoted by (☆) in the oxygen panel, suggests the existence of lithium-rich sulfate phases. The presence of lithium sulfate is confirmed by XRD analysis. Overall, the formation of distinct phases of nickel, manganese, cobalt and lithium that are physically separable suggests that selective sulfidation is a technically-viable pretreatment. It offers to shift the burden of selectivity in lithium ion battery recycling from energy intensive pyrometallurgical or hydrometallurgical chemical separations to more benign chemical pretreatments for physical methods[1,17]. In the following section, we explore selective sulfidation applied to copper recovery from copper smelting slags as a means to overcome the mineralogical barrier at low product grades by increasing the grade of recoverable sulfide phases.

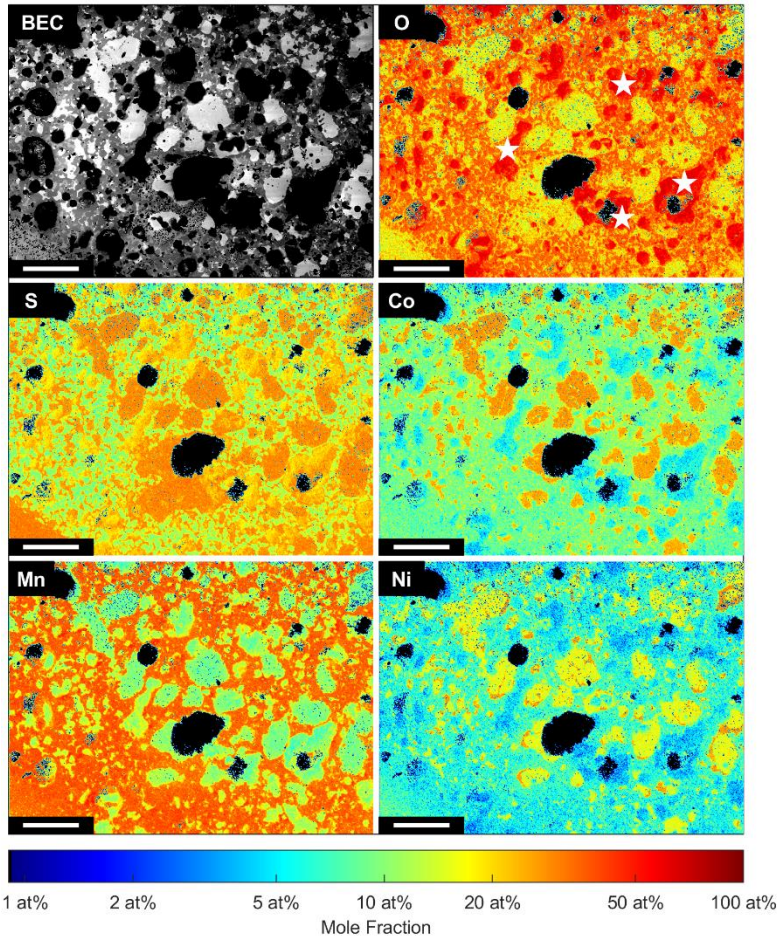

Figure 4: Selective sulfidation of synthetic nickel-manganese-cobalt oxide (NMC111) lithium ion battery cathode nucleates distinct nickel-rich, cobalt-rich, and manganese-rich phases on the order of 100-200 μm in size, as illustrated via EDS mapping for the region shown in the SEM/BEC image, large enough for liberation of Ni, Co, and Mn via comminution and physical separation. XRD analysis reveals the presence of lithium as a sulfate, possibly corresponding to oxygen-sulfur-rich, metal-deficient regions in the element maps, denoted by (☆) in the oxygen panel. Scale bars correspond to 200 μm. (Color images available online).

Selective Sulfidation for Copper Recovery from Slags

While electrification of the transportation sector continues to increase demand for battery metals[3], electrification of society is predicted to more broadly stress copper supplies[58], motivating efforts to increase recovery of copper from both primary and secondary sources. Presently, approximately 80% of the world's copper ore is produced from smelting of copper-iron-sulfide minerals[13]. For separation of iron from copper via matte smelting, the molten copper-iron-sulfide matte is contacted with a silica-rich slag phase. Following matte smelting, the slag contains approximately 75-90% fayalite, <10% alumina, <10% calcia, <4% magnesia, and 0.5-2.1% copper in the form of entrained sulfide matte particles and copper dissolved in fayalite[20]. Considering that smelters pay for

about 96% of the copper value when purchasing concentrate[59], there is a strong economic incentive to minimize and recover copper lost to the slag phase during matte smelting. Copper in the form of entrained matte particles is presently liberated from slags via comminution and physically separated[13], yet at copper grades less than 1%, the practical mineralogical barrier between chemical and physical separation begins to diminish. As shown in Figure 1 for copper recovery from slag at a grade of 0.5 wt%, energy needs for physical and chemical separation are predicted to be on the same order of magnitude. This calls into question the relative energetic effectiveness of selectivity in current physical separation methods. Meanwhile, the solubility of copper oxide in fayalite is approximately 1%[20], representing a significant fraction of copper in the slag that is inaccessible to recovery via physical separation without pretreatment.

Numerous pretreatments based on sulfidation have been explored to recover copper dissolved in fayalite phases of slag, generally utilizing roasting the slag in the presence of pyrite[60,61] or iron sulfate[62] to form leachable or floatable copper phases. As shown by ψ_{rxn} in Figure 2, the pure oxides of copper and iron are thermodynamically predicted to sulfidize at far lower sulfur to sulfur dioxide gas ratios than pure magnesia, alumina, and silica slag-formers. Under conditions where pure iron oxide sulfidizes, calcium is predicted to be stable as a sulfate. However, even if copper can be selectively precipitated as a sulfide via a selective sulfidation pretreatment, closing of the practical mineralogical barrier (Figure 1) at grades relevant to recover copper from fayalite slag phases suggests that the energy difference may be small between chemical separation and physical separation with pretreatment. To overcome the practical mineralogical barrier, a higher-grade phase may be used to serve as a collector for copper upon sulfidation pretreatment. This will allow copper to be liberated with this higher grade "collector" phase and thereby lower energy input. From the fayalite phase, iron may be co-sulfidized with copper, predicted to increase the total sulfide product grade in the slag for liberation and physical separation from approximately 0.5 wt% up to 40 wt% and reduce the energy burden from chemical separation at a grade of 0.5 wt% by three orders of magnitude (Figure 1).

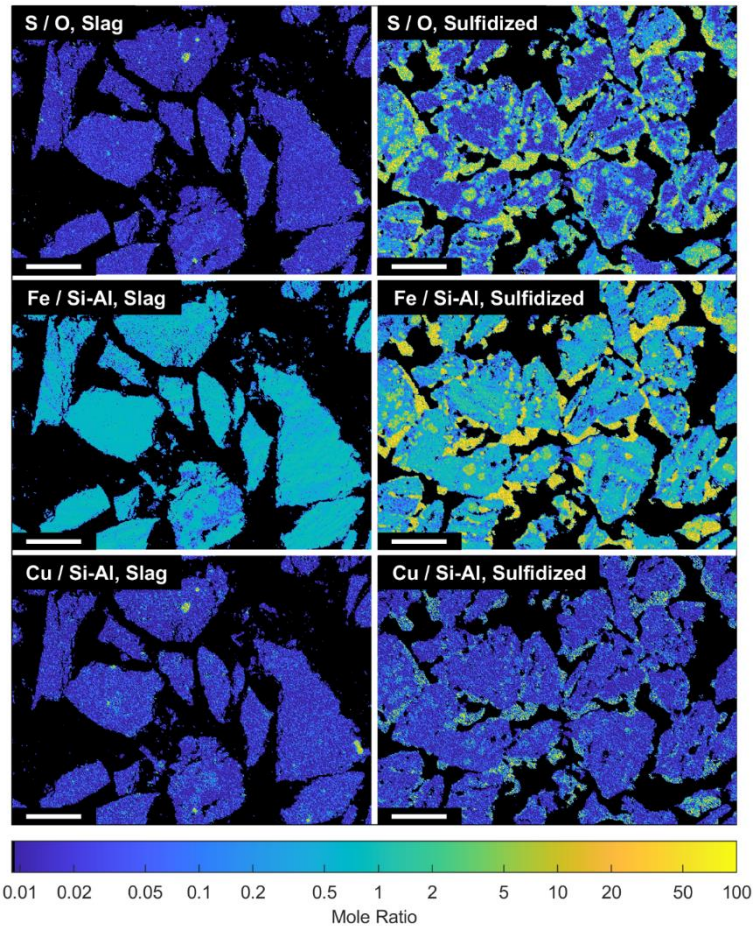

Figure 5: Selective sulfidation of copper smelter slag results in the nucleation of iron-rich sulfide phases, with copper preferentially partitioning into these new sulfide phases versus silicon and aluminum. Iron sulfide formed via selective sulfidation serves as a "collector" phase for copper, potentially supporting increased recovery of copper from slags via comminution and physical separation. Scale bars correspond to 100 μm. (Color images available online).

We conducted the selective sulfidation at 800 °C of copper and iron from copper smelter slag ground to a particle size of 90-212 μm, at a scale of 2 g, using vaporized elemental sulfur (S_x, 99.5% purity, Acros Organics) at a partial pressure of approximately 0.1 atm. The sulfur to sulfur dioxide gas ratio was approximately 10:1, following methods and reactor design described previously[33]. Here, the alumina reactor bed previously employed[33] was substituted for graphite to minimize interactions between slag phases and the reactor. Figure 5 show the SEM/EDS (SEM: JEOL JSM-6610LV, JEOL Ltd., EDS: Sirius SD detector, SGX Sensortech Ltd.) element maps detailing ratios of sulfur to oxygen, iron to silicon and aluminum, and copper to silicon and aluminum in the untreated and sulfidized copper smelter slag.

As shown in Figure 5, iron and copper are observed to preferentially segregate over silicon and aluminum to the sulfide phase, resulting in iron-copper-sulfide and aluminum-silicon oxide product phases. In the untreated slag, sulfide phases are observed to constitute a grade of approximately 1 wt%, increasing to approximately 16 wt% upon sulfidation. Product sulfide phases were observed to be on the order of 50 μm, large enough for effective liberation[22,23] and physical separation using standard industrial mineral processing methods[25,51]. The depletion of copper content from fayalite slag phases was difficult to quantify via SEM/EDS due to an abundance near the detection limit of the equipment. Further analysis will be needed to determine the conversion of solubilized copper in fayalite to sulfide and the partitioning of valuable trace elements such as cobalt and platinum group elements between oxide and sulfide phases. The use of an iron sulfide collector phase, formed in situ from sulfidation of iron from fayalite, allows the energetic burden of selectivity to be shifted from low product grades (~1 wt%) to higher grades (~16 wt%) via the selective sulfidation pretreatment. This indicates that the practical mineralogical barrier is widened, now in favor of lower-energy physical separation methods. The sulfide grade may be further increased toward 40% by increasing the sulfur to sulfur dioxide ratio in the reactor to improve the conversion of fayalite to iron sulfide. Meanwhile, excess heat produced from smelting of the iron-rich recovered copper sulfide may in turn be used to melt higher concentrations of gangue impurities in copper concentrate during smelting. This would facilitate the use of lower grade concentrates at a time of falling ore grades, while simultaneously increasing copper recovery[63].

Conclusions

Electrification-induced growth in demand for sustainably-sourced metallic elements drives efforts to reduce the energy use of materials separations in both primary and secondary production. A mineralogical barrier exists between the lower energy burden for physical separation of elements concentrated in distinct phases and the higher energy burden for chemical separation of elements mixed at the atomic scale. Through comparing the energy usage of industrial-scale materials separation processes, this difference in energy is generally found to range from approximately 200 kWh to 2,000 kWh per tonne of feed at product grades ranging between 1 wt% and 30 wt%. While this analysis does not replace detailed thermodynamic and life cycle assessments of individual materials systems, it illustrates that in general significant energy savings in material separation can be realized through the development of energy-efficient pretreatments that facilitate physical separation in place of chemical separation. Selective sulfidation is a potential pretreatment to partition metallic elements from multi-metal compounds and solid solutions into separate oxide and sulfide phases, allowing the burden of selectivity to be shifted from chemical to physical methods of separation. We demonstrate selective sulfidation of calcined rare earth magnets to partition iron and rare lanthanide elements into distinct, physically separable phases for recycling by physical separation. Similarly, we partition nickel, manganese, cobalt, and lithium from lithium ion battery cathodes into distinct, physically separable phases for lithium ion battery recycling by physical separation. Finally, we use selective sulfidation to form a dedicated sulfide collector phase for copper recovery from copper smelter slag, increasing the grade of copper-containing sulfide phases from approximately 1 wt% to approximately 16 wt%. For these recycling challenges, the selective sulfidation pretreatment facilitates the use of physical separations that are predicted to require 10-100x less energy than comparable chemical separations.

Acknowledgements

The authors wish to thank Marko Yakasovic for providing samples of copper smelter slag and Dr. Mary Elizabeth Wagner for insight pertaining to rare earth magnet thermodynamics and recycling.

References

1. Harper, G. *et al.* Recycling lithium-ion batteries from electric vehicles. *Nature* vol. 575 75–86 (2019).
2. Allanore, A. Electrocehmical engineering for commodity metals extraction. *Electrochem. Soc. Interface* **26**, 63–68 (2017).
3. Nguyen, R. T., Eggert, R. G., Severson, M. H. & Anderson, C. G. Global Electrification of Vehicles and Intertwined Material Supply Chains of Cobalt, Copper and Nickel. *Resour. Conserv. Recycl.* **167**, 105198 (2021).
4. Cheisson, T. & Schelter, E. J. Rare earth elements: Mendeleev's bane, modern marvels. *Science (80-.).* **363**, 489–493 (2019).
5. Olivetti, E. A., Ceder, G., Gaustad, G. G. & Fu, X. Lithium-Ion Battery Supply Chain Considerations: Analysis of Potential Bottlenecks in Critical Metals. *Joule* vol. 1 229–243 (2017).
6. Binnemans, K., Jones, P. T., Müller, T. & Yurramendi, L. Rare Earths and the Balance Problem: How to Deal with Changing Markets? *Journal of Sustainable Metallurgy* vol. 4 126–146 (2018).

7. Rötzer, N. & Schmidt, M. Decreasing Metal Ore Grades—Is the Fear of Resource Depletion Justified? *Resources* **7**, 88 (2018).
8. Norgate, T. & Jahanshahi, S. Low grade ores - Smelt, leach or concentrate? *Miner. Eng.* **23**, 65–73 (2010).
9. Wagner, M.-E. & Allanore, A. Chemical Thermodynamic Insights on Rare-Earth Magnet Sludge Recycling. *ISIJ Int.* **60**, 2339–2349 (2020).
10. Wang, M. Enthalpy of formation of LiNiO2, LiCoO2 and their solid solution, LiNi1−xCoxO2. *Solid State Ionics* **166**, 167–173 (2004).
11. Chang, K., Hallstedt, B. & Music, D. Thermodynamic and Electrochemical Properties of the Li−Co−O and Li−Ni−O Systems. *Chem. Mater.* **24**, 97–105 (2011).
12. Crundwell, F. K., Moats, M. S., Ramachandran, V., Robinson, T. G. & Davenport, W. G. *Extractive Metallurgy of Nickel, Cobalt, and Platinum-Group Metals*. (Elsevier, 2011).
13. Schlesinger, M. E., King, M. J., Sole, K. C. & Davenport, W. G. *Extractive Metallurgy of Copper*. (Elsevier, 2011). doi:10.1017/CBO9781107415324.004.
14. Zhao, B., Zhang, J. & Schreiner, B. *Separation Hydrometallurgy of Rare Earth Elements*. (Springer International Publishing AG Switzerland, 2016).
15. Skinner, B. J. A Second Iron Age Ahead? The distribution of chemical elements in the earth's crust sets natural limits to man's supply of metals that are much more important to the future of society than limits on energy. *Sci. Am.* **64**, 258–269 (1976).
16. Skinner, B. J. Earth resources (minerals/metals/ores/geochemistry/mining). *Proc. Natl. Acad. Sci. USA* **76**, 4212–4217 (1979).
17. Ciez, R. E. & Whitacre, J. F. Examining different recycling processes for lithium-ion batteries. *Nat. Sustain.* **2**, 148–156 (2019).
18. Zhang, Y. *et al.* Hydrometallurgical Recovery of Rare Earth Elements from NdFeB Permanent Magnet Scrap: A Review. *Met. 2020, Vol. 10, Page 841* **10**, 841 (2020).
19. Ahmed, S., Nelson, P. A., Gallagher, K. G., Susarla, N. & Dees, D. W. Cost and energy demand of producing nickel manganese cobalt cathode material for lithium ion batteries. *J. Power Sources* **342**, 733–740 (2017).
20. Gorai, B., Jana, R. K. & Premchand. Characteristics and utilisation of copper slag - A review. *Resour. Conserv. Recycl.* **39**, 299–313 (2003).
21. Fuerstenau, D. & Abouzeid, A.-Z. The energy efficiency of ball milling in comminution. *Int. J. Miner. Process.* **67**, 161–185 (2002).
22. King, R. P. A model for the quantitative estimation of mineral liberation by grinding. *Int. J. Miner. Process.* **6**, 207–220 (1979).
23. Finch, J. A. & Petruk, W. Testing a solution to the King liberation model. *Int. J. Miner. Process.* **12**, 305–311 (1984).
24. Taylor, L., Skuse, D., Blackburn, S. & Greenwood, R. Stirred media mills in the mining industry: Material grindability, energy-size relationships, and operating conditions. *Powder Technol.* **369**, 1–16 (2020).
25. de Bakker, J. Energy Use of Fine Grinding in Mineral Processing. *Metall. Mater. Trans. E* **1**, 8–19 (2014).
26. A.Curry, J., J.L.Ismay, M. & J.Jameson, G. Mine operating costs and the potential impacts of energy and grinding. *Miner. Eng.* **56**, 70–80 (2014).
27. Harris, C. T., Peacey, J. G. & Pickles, C. A. Selective sulphidation and flotation of nickel from a nickeliferous laterite ore. *Miner. Eng.* **54**, 21–31 (2013).
28. Han, J., Liu, W., Wang, D., Jiao, F. & Qin, W. Selective Sulfidation of Lead Smelter Slag with Sulfur. *Metall. Mater. Trans. B* **47**, 344–354 (2015).
29. Han, J. *et al.* Selective Sulfidation of Lead Smelter Slag with Pyrite and Flotation Behavior of Synthetic ZnS. *Metall. Mater. Trans. B* **47B**, 2400–2410 (2016).
30. Han, J. *et al.* Selective Sulfidation of Lead Smelter Slag with Pyrite and Flotation Behavior of Synthetic ZnS. *Metall. Mater. Trans. B Process Metall. Mater. Process. Sci.* **47**, 2400–2410 (2016).
31. Ke, Y. *et al.* Sulfidation behavior and mechanism of zinc silicate roasted with pyrite. *Appl. Surf. Sci.* **435**, 1011–1019 (2018).
32. Zhuo-yue, L. *et al.* Recovery of Zn, Pb, Fe and Si from a low-grade mining ore by sulfidation roasting-beneficiation-leaching processes. *J. Cent. South Univ.* **27**, 37–51 (2020).
33. Stinn, C. & Allanore, A. Selective Sulfidation and Electrowinning of Nickel and Cobalt for Lithium Ion Battery Recycling. in *Ni-Co 2021: The 5th International Symposium on Nickel and Cobalt* 99–110 (Springer Science and Business Media Deutschland GmbH, 2021). doi:10.1007/978-3-030-65647-8_7.
34. Adham, K. & Lee, C. Fluid Bed Roasting of Metal Ores and Concentrates for Arsenic Removal. in *Towards*

Clean Metallurgical Processing for Procfit, Social, and Environmental Stewardship 109–116 (2012).
35. U.S. Geological Survey. *Mineral Commodity Summaries 2021*. (2021).
36. Afanasiev, P. *et al.* Preparation of the mixed sulfide Nb2Mo3S10 catalyst from the mixed oxide precursor. *Catal. Letters* **64**, 59–63 (2000).
37. Akila, R., Jacob, K. T. & Shukla, A. K. Gibbs Energies of Formation of Rare Earth Oxysulfides. *Metall. Trans. B* **18B**, 163–168 (1987).
38. Pourbaix, M. J. N. & Rorive-Bouté, M. C. M. Graphical study of metallurgical equilibria. *Discuss. Faraday Soc.* **4**, 139–154 (1948).
39. Kellogg, H. H. A Critical Review of Sulfation Equilibria. *Trans. Metall. Soc. AIME* **230**, 1622–1634 (1964).
40. Fleet, M. E. & MacRae, N. D. Sulfidation of Mg-rich olivine and the stability of niningerite in enstatite chondrites. *Geochim. Cosmochim. Acta* **51**, 1511–1521 (1987).
41. Fleet, M. E., Tronnes, R. G. & Stone, W. E. Partitioning of platinum group elements in the Fe-O-S System to 11 GPa and their fractionation in the mantle and meteorites. *J. Geophys. Res. Solid Earth* **96**, 21949–21958 (1991).
42. Bataleva, Y. V., Palyanov, Y. N., Borzdov, Y. M. & Sobolev, N. V. Sulfidation of silicate mantle by reduced S-bearing metasomatic fluids and melts. *Geology* **44**, 271–274 (2016).
43. Goldschmidt, V. M. The principles of distribution of chemical elements in minerals and rocks. The seventh Hugo Müller Lecture, delivered before the Chemical Society on March 17th, 1937. *J. Chem. Soc.* 655–673 (1937) doi:10.1039/JR9370000655.
44. Holser, W. T. & Kaplan, I. R. Isotope geochemistry of sedimentary sulfates. *Chem. Geol.* **1**, 93–135 (1966).
45. Bailey, G. *et al.* Review and new life cycle assessment for rare earth production from bastnäsite, ion adsorption clays and lateritic monazite. *Resour. Conserv. Recycl.* **155**, 104675 (2020).
46. K Lee, J. C. & Wen, Z. Pathways for greening the supply of rare earth elements in China. *Nat. Sustain.* **1**, 598–605 (2018).
47. Jowitt, S. M., Werner, T. T., Weng, Z. & Mudd, G. M. Recycling of the rare earth elements. *Curr. Opin. Green Sustain. Chem.* **13**, 1–7 (2018).
48. Firdaus, M., Rhamdhani, M. A., Durandet, Y., Rankin, W. J. & McGregor, K. Review of High-Temperature Recovery of Rare Earth (Nd/Dy) from Magnet Waste. *J. Sustain. Metall. 2016 24* **2**, 276–295 (2016).
49. Rasheed, M. Z. *et al.* Review of the Liquid Metal Extraction Process for the Recovery of Nd and Dy from Permanent Magnets. *Metall. Mater. Trans. B 2021 523* **52**, 1213–1227 (2021).
50. Yin, X. *et al.* Rare earth separations by selective borate crystallization. *Nat. Commun.* **8**, (2017).
51. Corin, K. C., McFadzean, B. J., Shackleton, N. J. & O'Connor, C. T. Challenges Related to the Processing of Fines in the Recovery of Platinum Group Minerals (PGMs). *Miner. 2021, Vol. 11, Page 533* **11**, 533 (2021).
52. Cohen-Adad, M. T. *et al.* Gadolinium and Yttrium Borates: Thermal Behavior and Structural Considerations. *J. Solid State Chem.* **154**, 204–213 (2000).
53. Dunn, J. B., Gaines, L., Sullivan, J. & Wang, M. Q. Impact of Recycling on Cradle-to-Gate Energy Consumption and Greenhouse Gas Emissions of Automotive Lithium-Ion Batteries. *Environ. Sci. Technol.* **46**, 12704–12710 (2012).
54. Korkmaz, K., Alemrajabi, M., Rasmuson, Å. & Forsberg, K. Recoveries of Valuable Metals from Spent Nickel Metal Hydride Vehicle Batteries via Sulfation, Selective Roasting, and Water Leaching. *J. Sustain. Metall.* **4**, 313–325 (2018).
55. Shi, J. *et al.* Sulfation Roasting Mechanism for Spent Lithium-Ion Battery Metal Oxides Under SO2-O2-Ar Atmosphere. *JOM* **71**, 4473–4481 (2019).
56. Bastanov, S. S., Ryabinina, O. I., Obzherina, K. F. & Derbeneva, S. S. On the Chemical Structure of Manganese Oxysulfides. *Bull. Acad. Sci. USSR, Div. Chem. Sci.* **17**, 6–11 (1968).
57. Liu, M. *et al.* Flower-like manganese-cobalt oxysulfide supported on Ni foam as a novel faradaic electrode with commendable performance. *Electrochim. Acta* **191**, 916–922 (2016).
58. Schipper, B. W. *et al.* Estimating global copper demand until 2100 with regression and stock dynamics. *Resour. Conserv. Recycl.* **132**, 28–36 (2018).
59. Bustillo, M. *Mineral Resources: From Exploration to Sustainable Assessment*. (2018).
60. Guo, Z., Zhu, D., Pan, J. & Zhang, F. Mechanism of Mineral Phase Reconstruction for Improving the Beneficiation of Copper and Iron from Copper Slag. *JOM 2016 689* **68**, 2341–2348 (2016).
61. Tümen, F. & Bailey, N. T. Recovery of metal values from copper smelter slags by roasting with pyrite. *Hydrometallurgy* **25**, 317–328 (1990).
62. Altundoğan, H. S. & Tümen, F. Metal recovery from copper converter slag by roasting with ferric sulphate.

Hydrometallurgy **44**, 261–267 (1997).
63. Rush, L. T. Thesis. (Massachusetts Institute of Technology).